

Original Research Article

Evaluation of MRI as diagnostic and classification tool for brachial plexus injuries cases.

Abstract

The incidence of the brachial plexus injuries is increased due to increase in sport and motor vehicle accidents. Detailed clinical examination is followed by MR imaging. The study was conducted on 30 patients of BPI. Patients with flail upper limbs and suspected root avulsions would undergo immediate MRI, while those without these indications would undergo MRI after a delay of 4-6 weeks. MRI aids in distinguishing between pre- and post-ganglionic or mixed injuries, particularly in cases where assessing both types of injuries presents difficulties. This is important as timing and type of surgery depends on whether the injury is pre- or postganglionic. We recommend MRI scan for the whole upper limb to assess edematous muscles, and pattern of the diaphragm movements. Contrast studies can also be added if not contraindicated.

Keywords : brachial plexus injuries, MRI imaging, Motor vehicle accidents, atrophy.

Introduction:

The upper extremities are innervated by the brachial plexus. Motor vehicle accidents are major source of injury though sports, radiation injury etc also contribute. The causes of the BPI are motor vehicles, sports, radiation, and labour (neonates) injuries. Detailed clinical examination is followed by MR imaging. The MRI is important diagnostic tool to classify injuries into preganglionic and post ganglionic injuries as well as identify the grade of the injuries and obscure injuries related to edema and atrophy of the muscles. (Sunderland classification – table 1)

Methods:

The study was conducted on 30 patients of BPI. MRI was done on 3 Tesla system (GE Healthcare Discovery 750W with GEM Suite, Milwaukee, WI, USA) using head-neck forty coil. Axial T2W (TE=114ms, TR=4800ms, FOV=22cm, slice thickness=5mm, spacing=1mm, frequency=512, bandwidth=50), coronal 3D/STIR (TE=102ms, TR=7000ms, FOV=40cm, slice thickness=2mm, spacing=0, frequency=256, band width=35.71), coronal T1W (TE=7ms, TR=456ms, FOV=22cm, slice thickness=4mm, spacing=0, frequency=352, band width=62.5), STIR neurography (TE=90.9ms, TR=16081.3ms, FOV=40cm, slice thickness=3mm, spacing=0, frequency=100, band width=250), and DW neurography (TE=73.8ms, TR=7000ms, FOV=30cm, slice thickness=4mm, spacing=0.5mm, frequency=100, band width=190) sequences were done. In addition, oblique sagittal T2 fat sat (TE=110ms, TR=5885ms, FOV=25cm, slice thickness=4mm, spacing=1mm, frequency=288, band width=31.25)

sequence was done on shoulder ipsilateral to injured brachial plexus, axial STIR (TE=42ms, TR=5465ms, FOV=35cm, slice thickness=4mm, spacing=0.5mm, frequency=352, band width=41.67) of ipsilateral arm, sagittal T2W (TE=76ms, TR=3105ms, FOV=16cm, slice thickness=2.5mm, spacing=0.2mm, frequency=288, band width=35.7) of cervical spine and axial cube T2 (TE=90mm, TR=1360mm, FOV=24cm, slice thickness=1.6mm, spacing=0, frequency=288, band width=83.33) of cervical spine were done.

Location of injury was identified, whether the injury was at root, trunk, division, cord or terminal branch level and whether it was pre- and/or postganglionic. Further, injury was graded

according to Sunderland classification (Table 1). MRI findings were correlated with clinical examination at the time of injury/MRI and on follow-up at three months.

Results:

The study included a total of 30 patients, comprising 26 males and 4 females, with ages ranging from 11 days to 58 years and a mean age of 29.4 ± 12.09 years. Among these patients, 14 had left-sided injuries, 12 had right-sided injuries, and 4 had bilateral injuries. Nerve roots were involved in 18 cases, trunks in 17 cases, divisions in 5 cases, and there was no direct injury to the brachial plexus in one patient. Ten patients exhibited preganglionic injuries, 17 had postganglionic injuries, and three had both pre- and postganglionic injuries.

Specifically, C5 nerve root was involved in 21 patients, C6 in 27 patients, C7 in 18 patients, C8 in 19 patients, and T1 in 14 patients. Grade I injuries were observed in three patients, grade III in nine patients, and grade V in eight patients, with 10 patients exhibiting multiple grades of injuries. Interestingly, no isolated grade II and IV injuries were seen in the study cohort.

The correlation between MRI findings and clinical presentation was found to be excellent. Out of 30 cases, 23 showed total correlation, while partial correlation was observed in seven cases. Among the patients, six demonstrated complete recovery, six showed partial recovery, three exhibited minimal recovery, and 15 showed no recovery. Notably, patients with lower grades of injury (grade I/II) tended to show complete recovery, whereas those with higher grades and extensive injury tended to exhibit minimal or no recovery.

Figure Legends:

Fig 1

(a) 3D T2W/STIR coronal images showing slight thickening and hyperintensity of left C5 & C6 postganglionic roots and upper trunk

(b) T2W/STIR coronal image showing edema in left supraspinatus and infraspinatus muscles

Fig 2

(a) 3D T2W/STIR coronal image showing pseudomeningocele at right C6 root (white arrow)

(b & c) Coronal diffusion weighted image & negative image showing kinking of Posterior cord laterally (there was healed fracture rib at this site) (blue arrow) and discontinuity and end neuroma at proximal fragment (red arrow) at medial cord

(d) T1W axial image showing atrophy of infraspinatus, subscapularis, pectoralis major and minor

Fig 3

(a) Coronal diffusion neurography showing normal brachial plexuses

(b) T2W/SPIR axial image showing edema and atrophy of right serratus anterior muscle (arrow)

Fig 4

(a, b & c) 3D T2W/STIR coronal, T2W sagittal cervical spine, coronal diffusion

neurography show pseudomeningocele s/o preganglionic injury to left C6, C7, C8 & T1 nerve roots, thickening and irregularity of left postganglionic C6, C7, C8 and T1 nerve roots and left middle and lower trunks

(d) T2W/STIR coronal image showing edema of supraspinatus, infraspinatus, fracture left upper ribs and left pleural effusion

Fig 5

(a) T2W/STIR coronal image showing pseudomeningocele at right C7 nerve root level (C6-C7 neural foramen)

(b) T2W/STIR coronal image showing discontinuity of postganglionic C5 (red arrow) and C6 (yellow arrow) nerve roots

(c) T2W/STIR sagittal image showing thickening, hyperintensity and blurred fascicles of lateral, posterior and medial cords

(d) T2W/STIR oblique sagittal image showing edema of supraspinatus, infraspinatus, subscapularis and teres minor muscles

(e) T2W axial image showing atrophy of pectoralis major, minor and also infraspinatus and subcapularis muscles

Fig 6

(a & b) 3D T2W/STIR coronal image and its negative showing hyperintensity and thickening of B/L C5, C6, C7 & C8 postganglionic roots and neuroma in continuity in right lateral cord distally (arrow)

(c) T2W/STIR oblique sagittal image showing slight denervation edema in right supraspinatus, infraspinatus, teres minor and deltoid muscles

(d) T2W/STIR axial image showing edema of biceps brachii muscle (arrow)

Fig 7

(a) T2W axial image showing pseudomeningocele at left D1-D2 neural foramen (arrow) (preganglionic injury D1)

(b & c) 3D T2W/STIR and diffusion neurography coronal images showing thickening, irregularity and hyperintensity of left C5 nerve root and neuroma in continuity (arrow) in left C7 postganglionic root

(d) Negative image of diffusion neurography coronal image showing normal cords on right side (red arrow) and discontinuous cords on left side (black arrow)

(e) T2W/STIR coronal image showing edema in left supraspinatus and subscapularis

muscles

Fig 8

(a & b) 3D T2W/STIR coronal image and its negative showing entanglement and probable discontinuity of left upper and lower trunk with a small (5mm) gap in lower trunk

(arrow)

(c) T2W?STIR oblique sagittal image showing edema in supraspinatus, infraspinatus with tear in superior aspect of subscapularis muscle

Fig 9

T1W coronal image showing involvement of left brachial plexus by carcinoma larynx

Fig 10

(a & b) Coronal diffusion neurography and its negative image showing indentation of right brachial plexus by cervical rib

(c) T1W oblique coronal image showing gross atrophy of supraspinatus, infraspinatus and subscapularis

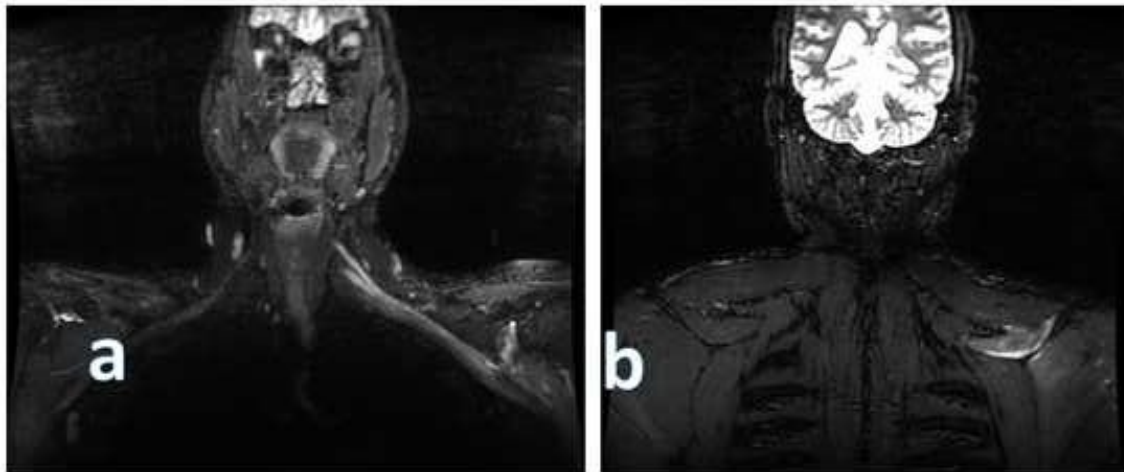


Fig.1

c

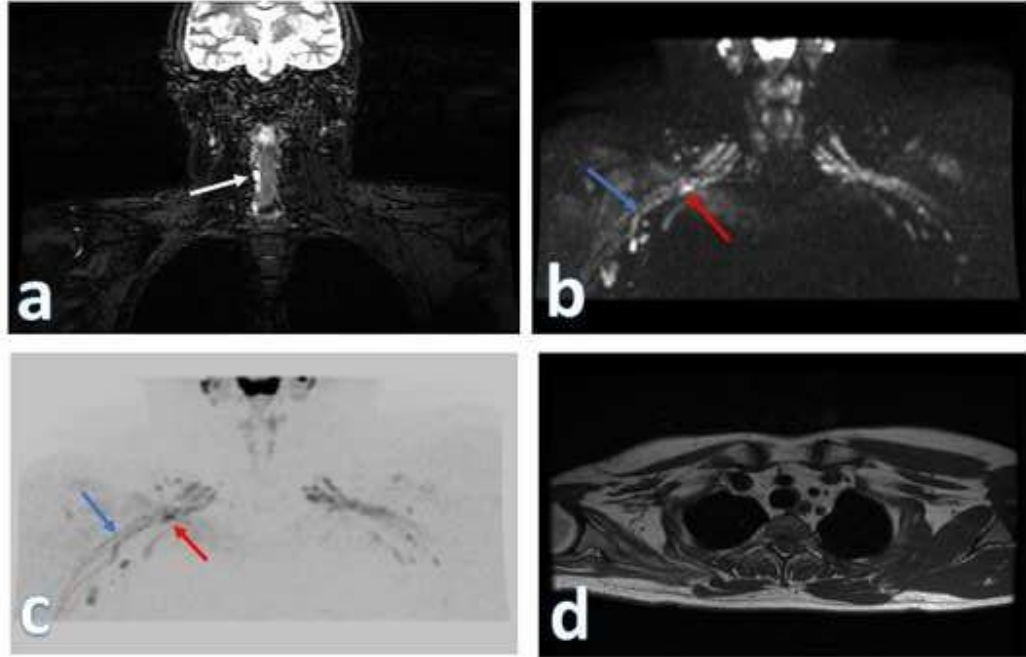


Fig.2

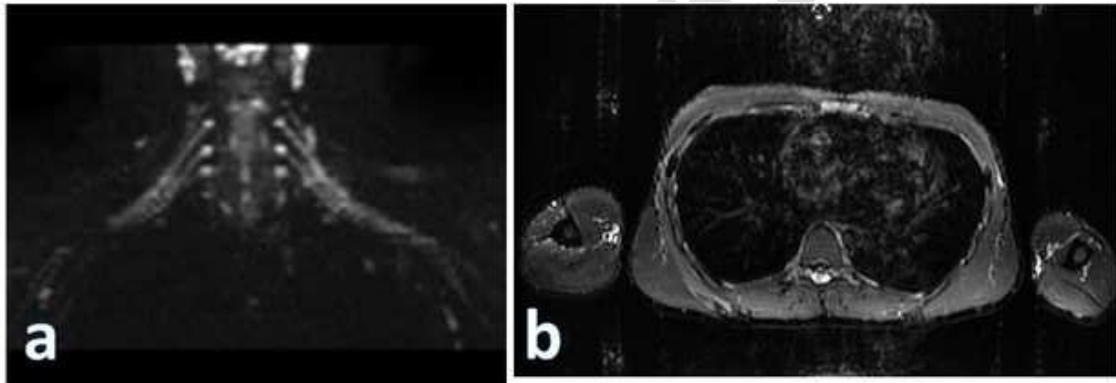


Fig.3

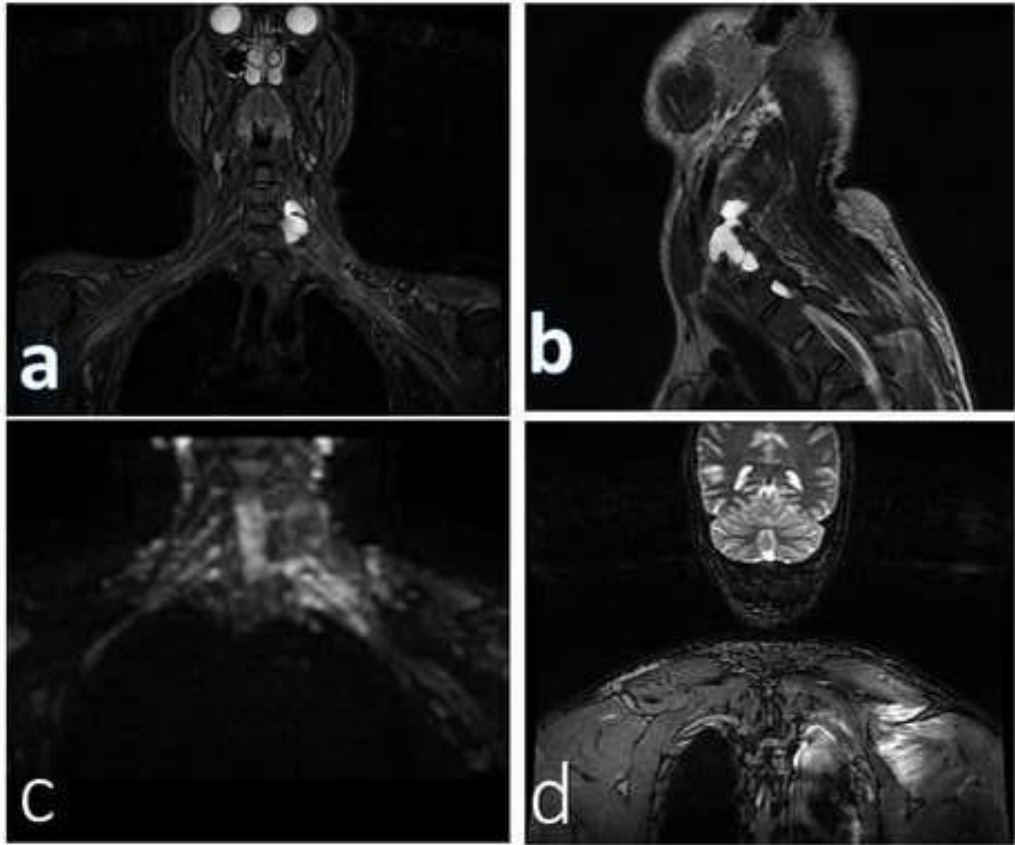


Fig.4

UNDER PEE

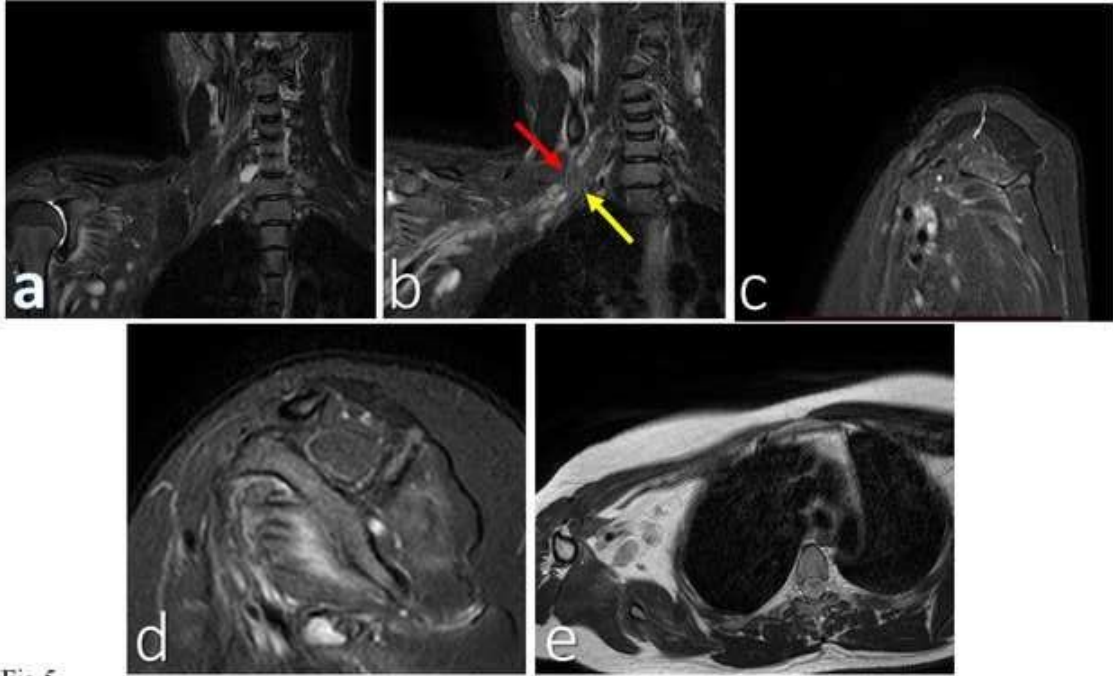


Fig.5

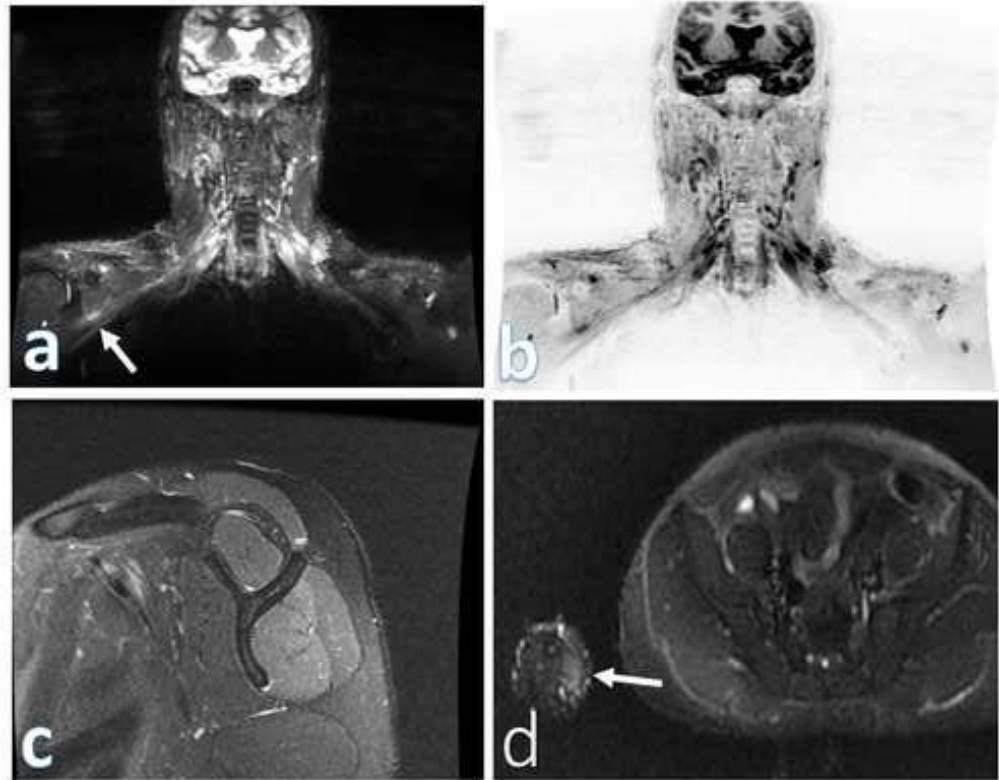


Fig.6

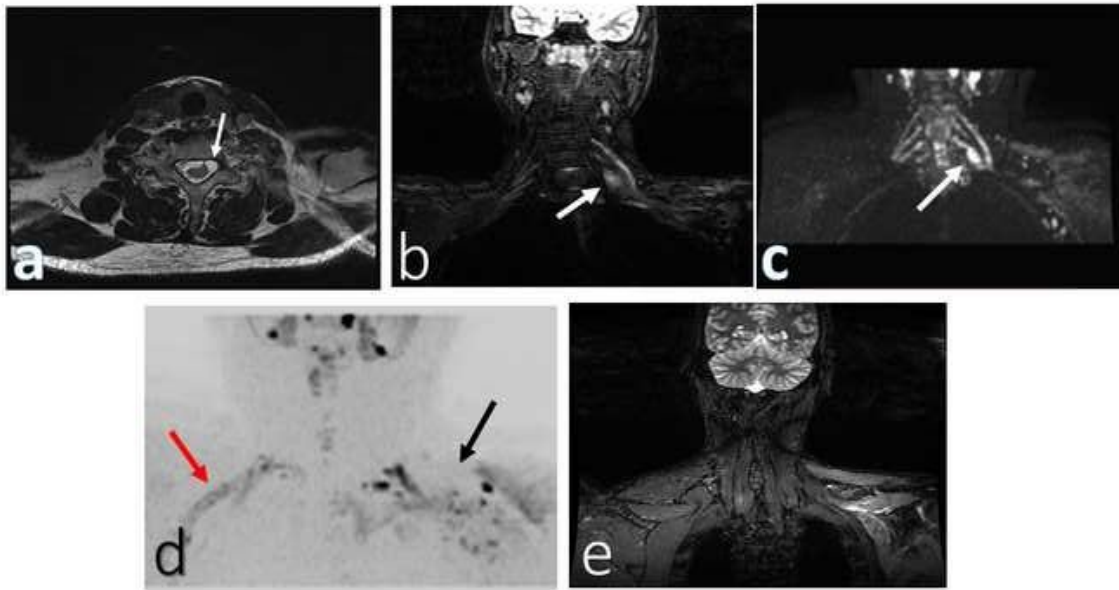


Fig.7

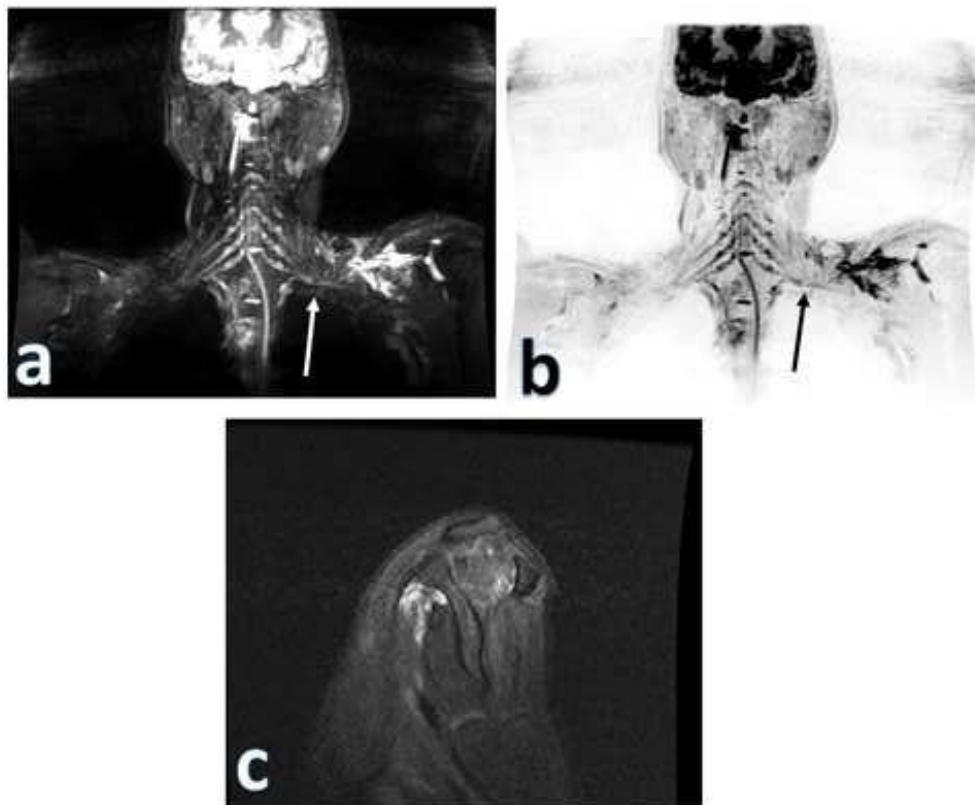


Fig.8

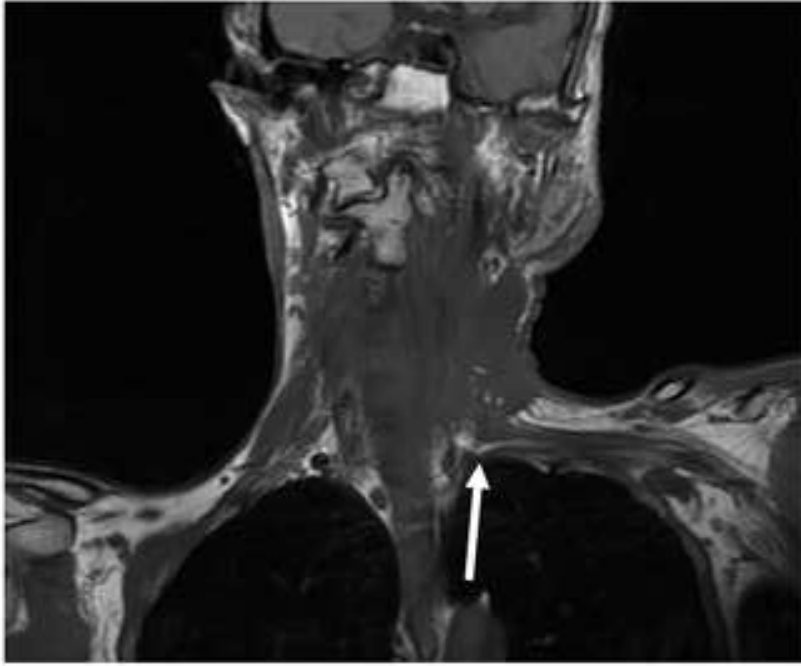


Fig.9

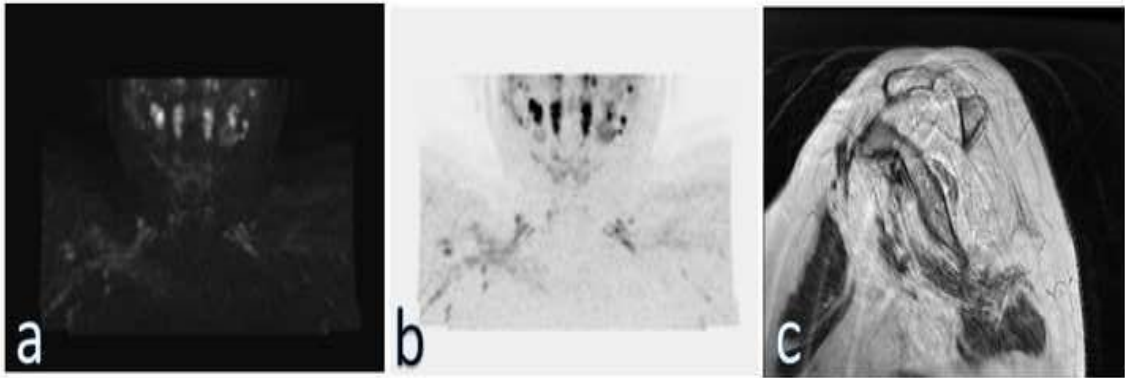


Fig.10

Degree of nerve injury	MRN (signal intensity)	Recovery potential	Surgery
I Neurapraxia	Nerve-increased T2 Signal intensity Muscle-Normal	Full	None
II Axonotmesis	Nerve-increased T2 signal intensity and diffusely enlarged	Full	None
III	Fascicles-enlarged or effaced due to edema Muscles-denervation	Usually slow, incomplete etc	None or Neurolysis
IV NIC-neuroma in continuity	Nerve-focally enlarged with heterogeneous signal intensity. Underlying diffuse abnormality ± fascicles disrupted with heterogeneous SI-NIC Muscles-denervation	Poor tone	Nerve repair, graft or transfer
V Neurotmesis	Complete nerve discontinuity ± hemorrhage and fibrosis in the nerve gap and end-bulb neuroma proximally. Epineurial thickening Muscles-denervation	None	Nerve repair, graft or transfer

Degree of nerve injury	MRN (signal intensity)	Recovery potential	Surgery
VI Mixed injury (I to V)	Variable findings along the circumferential segment of the nerve (I-V) with heterogeneous signal intensity due to fibrosis	Variable, can be poor to none	Neurolysis, nerve repair, graft or transfer

Table 1: Table showing degrees of postganglionic nerve injuries (Sunderland classification)

Discussion:

The findings of this study underscore the importance of accurately classifying brachial plexus injuries (BPI) based on factors such as extent of injury, site of injury, grade of injury, associated injuries, and status of surrounding structures. Such classification is crucial for determining appropriate treatment strategies (conservative vs. surgical) and predicting prognosis.

MRI emerged as a valuable tool for distinguishing between pre- and postganglionic injuries, especially in cases where both types of injuries were present, thus aiding in surgical decision-making. Additionally, detailed examination and diagnostic procedures such as electromyography (EMG) and nerve conduction velocity studies were instrumental in localizing the level of lesion, assessing severity of axon loss, and monitoring recovery progress.

Moreover, the study highlighted the significance of timely MRI imaging, with specific indications for urgent imaging in certain clinical scenarios. MRI not only facilitated accurate diagnosis but also influenced treatment decisions, as evidenced by cases where alternative pathologies were identified, leading to modified treatment approaches.

Despite its utility, the study acknowledges limitations such as small sample size and the need for comprehensive imaging protocols to assess the full extent of injury, including forearm

and hand muscles, diaphragm movements, and the potential benefits of contrast-enhanced MRI. Recommendations for refining imaging protocols to enhance diagnostic accuracy are provided based on study observations.

In conclusion, the judicious integration of various diagnostic modalities, including MRI, EMG, and nerve conduction studies, plays a pivotal role in effectively managing BPI by informing treatment decisions, predicting outcomes, and optimizing patient care. Further research with larger sample sizes and refined imaging protocols is warranted to validate these findings and improve clinical practice in the management of BPI.

Conclusion:

MRI is very useful in proper diagnosis and assessment of extent of brachial plexus injury helping in deciding treatment (conservative or surgical) and timing of surgery. MRI also assesses surrounding normal muscles and nerves in terms of their suitability for nerve transfer.

Compliance with ethical requirements:

All procedures followed were in accordance with the ethical standards of the responsible committee on human experimentation (institutional and national) and with the Helsinki Declaration of 1975, as revised in 2008 (5). Informed consent was obtained from all patients for being included in the study. This article does not contain any studies with animal subjects.

Consent :

Written informed consent was obtained from the patients for publication and any accompanying images. A copy of the written consent is available for review by the Editor-in-Chief of this journal on request.

References:

1. Mallouhi A, Marik W, Prayer D, Kainberger F, Bodner G, Kasprian G. 3 T MRI tomography of the brachial plexus: structural and microstructural evaluation. *Eur J Radiol* 2012; 81:2231-2245.
2. Yoshikawa T, Hayashi N, Yamamoto S, Tajiri Y, Yoshioka N, Masumoto T, et al. Brachial plexus injury: clinical manifestations, conventional imaging findings, and the latest imaging techniques. *Radiographics* 2006;26(1):S133-S43

3. Siqueira MG, Martins RS. Surgical treatment of adult traumatic brachial plexus injuries. *Arq Neuropsiquiatr* 2011;69(3):528-35
4. Moran SL, Steinmann SP, Shin AY. Adult brachial plexus injuries: Mechanism, patterns of injury, and physical diagnosis. *Hand Clin* 2005;21:13-24
5. Warren J, Gutmann L, Figuerca AS Jr, Bloor BM. Electromyographic changes of brachial plexus root avulsion. *J Neurosurg* 1969;31:137-40.
6. Park HR, Lee GS, Kim S, Chang JC. Brachial plexus injury in adults. *The Nerve* 2017;3(1):1-11
7. Carlstedt T, Anand P, Hallin R, Misra PV, Noren G, Seferlis T. Spinal nerve root repair and reimplantation of avulsed ventral roots into the spinal cord after brachial plexus injury. *J Neurosurg* 2000;93:237-47
8. Sakellariou VL, Badilas NK, Stavropoulos NA, Mazis G, Kotoulas HK, Kyriakopoulos S, et al. Treatment options for brachial plexus injuries. *ISNR Orthopedics* 2014;2014:1-10
9. Duijnisveld BJ, Henseler JF, Reijnierse M, Fiocco M, Kan HE, Nelissen RGHH. Quantitative Dixon MRI sequences to relate muscle atrophy and fatty degeneration with range of motion and muscle force in brachial plexus injury. *Magn Reson Imaging* 2017;36:98-104
10. Viguie CA, Lu DX, Huang SK, Rengen H, Carlson BM. Quantitative study of the effects of long term denervation on the extensor digitorum longus muscle of the rat. *Anat Rec* 1997;248:346-54
11. Kato N, Htut M, Taggart M, Carlstedt T, Birch R. The effects of operative delay on the relief of neuropathic pain after injury to the brachial plexus: a review of 148 cases. *J Bone Joint Surg Br* 2006;88:256-9
12. Chhabra A, Thakkar RS, Andreisek G, Chalian M, Belzberg AJ, Blakeley J, et al. Anatomic MR imaging and functional diffusion tensor imaging of peripheral nerve tumors and tumorlike conditions. *AJNR Am J Neuroradiol* 2013; 34(4): 802-7.